Transport of Water into the Lower Mantle: The Role of Stishovite

Wendy R. Panero [a]
Laura Robin Benedetti [b]
Raymond Jeanloz [c]

[a] Department of Geological Sciences
    University of Michigan
    Ann Arbor, MI 48109-1063
[b] Department of Physics
[c] Department of Earth and Planetary Science
    University of California
    Berkeley, CA 94720

When subjected to lower-mantle pressures and temperatures, natural "anhydrous" basalt containing 0.2 wt% H_2O forms a phase assemblage in which SiO_2 stishovite is a significant carrier of hydrogen (up to 500 ppm H_2O by weight, as hydroxide), whereas the coexisting (Mg, Fe, Al, Ca)SiO_3 perovskite appears not to be (upper bound of 50 ppm (wt) H_2O). Contrary to the devolatilization characteristically observed at lower pressures, we find that the abundance of H_2O in residual stishovite increases from ~100 ppm to ~400 ppm by weight upon partially melting the high-pressure mineral assemblage at 28-60 GPa. We infer that the trace concentration of Al within residual stishovite increases upon partial melting, thereby increasing the coupled abundance of H in this crystalline phase. The "anhydrous" component of subducted oceanic crust can thus recycle a significant amount of water into the lower mantle over the age of the Earth, with subducted stishovite potentially returning ~10^2 times the amount of water present in today's atmosphere.

Introduction

The distribution of volatile molecules (e.g., H_2O, CO_2) in the mantle affects the chemical and physical evolution of the Earth [e. g., *Righter and Drake, 1999; Kuramoto and Matsui, 1996*]. Degassing of the mantle currently occurs predominantly at mid-ocean ridges, where basaltic crust containing about 0.07-0.6 wt% water is erupted [*Delany et al., 1978*]. Assuming a peridotite/melt OH partitioning coefficient of 0.01, the source region for the mid-ocean ridge basalts (MORB) that form the sub-oceanic crust should contain at least 80-950 ppm H_2O by weight, as some of the water may be released directly to the ocean [*Ito et al., 1983*]. However, the nature of the MORB source region provides little constraint on the volatile content of the bulk of the mantle (e.g., the lower mantle). Specifically, if portions of the mantle have remained undepleted by partial melting or have received recycled volatiles from returning subducted material, it is likely that these regions contain greater abundances of volatile components than the MORB source region. The nature of any segregated material in the mantle remains a subject of debate both with respect to global geochemical inventories as well as the volatile content of the mantle [e.g., *Tackley 2000*; *Albarède and van der Hilst,* 1999*; Kellogg et al., 1999*].

Seismic evidence for subducting slabs penetrating into the lower mantle [e.g., *Van der Voo et al., 1999; Grand et al., 1997*] suggests a means of returning volatile components to the deep interior via plate tectonics. However, it is difficult to constrain observationally the amount of water subducted to great depth, relative to that returned to the surface through arc volcanism [*Peacock, 1990*]. Instead, attempts have been made to determine water budgets experimentally, by examining the stability of hydrous minerals with respect to pressure and temperature [*e.g. Schmidt and Poli, 1998*]. If they survive to great depth, hydrous minerals can recycle large amounts of water relative to the amount present in the current oceans and atmosphere. For example, hydrated basalt forms lawsonite in cold slabs [*Schmidt and Poli, 1998*], which may transform into other dense, hydrous, magnesium silicates upon subduction to greater depths [*Williams and Hemley, 2001*]. This could be a dominant process for water recycling to the deep mantle in regions where fast, old and

therefore cold slabs are subducting.

Inconclusive evidence about the stability of any of these hydrous phases under mantle conditions and realistic compositions leaves this mode of returning volatile elements into the deep Earth uncertain. Only a small fraction (less than 10%) of subducted, basaltic crust has ever undergone significant alteration through interaction with the oceans [*Alt and Teagle, 2000*]. The remaining unaltered basaltic material only contains water directly resulting from partial melting of the upper mantle. Therefore, 0.07-0.6 wt% H_2O is incorporated into the nominally "anhydrous" oceanic crust during its formation, directly through partial melting of the upper mantle [*Delany et al., 1978*]. This water is not expected to be released in the mantle wedge upon subduction because it is not contained in hydrous phases, but rather is incorporated into anhydrous minerals such as olivine, diopside, plagioclase, and garnet. Natural pyroxenes have been shown to contain up to 500 ppm H_2O [*Bell and Rossman, 1992*], while clinopyroxenes have been found with an excess of 1000 ppm H_2O [*Thompson 1992*]. Olivine and garnet are generally found to contain less water, but the solubility of water in these phases increases with pressure [*Lu and Keppler*, 1997]; pyrope garnets incorporate up to 470 ppm water at about 10 GPa and 1100 K, the expected point of break down of phengite [*Schmidt* 1996]. It thus appears inevitable that an unaltered basaltic crust can carry water down to the transition zone without undergoing dehydration because of the *increasing* stability of hydrogen in the anhydrous minerals with pressure.

The important point is that "anhyrdous" assemblages, such as those formed from MORB, do contain finite amounts of hydrogen as a trace, not stochiometric, component of the minerals. Over geological time periods, the presence of even trace amounts of hydrogen in subducted slabs can have a profound influence on the history of the Earth's water. Furthermore, when considering the effect on the dynamics of the mantle, hydrogen concentrations at the parts per million level can have significant effects on the rheology and evolution of the Earth's interior.

The potential for storage of water in "anhydrous" high-pressure phases found in subducted slabs has been documented for conditions corresponding to depths of ~300 km (stishovite) [*Pawley et al., 1993*], the transition zone (e.g., garnet and ringwoodite) [*Lu and*

Keppler, 1997; Bolfan-Casanova et al., 2000] and the top of the lower mantle (Mg-perovskite) [*Meade et al., 1994; Murakami et al., 2002*]. Prior studies have not documented the hydrogen content of the multi-phase assemblage formed from MORB at deep-mantle conditions, nor have they addressed the change in hydrogen content of lower-mantle crystalline phases in response to partial melting, however.

We therefore examine the stability of hydrogen in the high-pressure assemblage formed from MORB, documenting the properties of a natural sample of oceanic crust at deep-mantle conditions. In anhydrous (unaltered) basalt, stishovite forms at and above 10 GPa in association with garnet, the primary mineral (> 50% of the assemblage by volume) between 12 and 27 GPa. At lower-mantle pressures, the phase assemblage consists of stishovite plus a Ca-Mg-Fe-Al orthorhombic perovskite (OPv II) at temperatures below ~2500 K [*Funamori et al., 2001*]. The OPvII phase is distinct from the orthorhombic-perovskite phase of $(Mg, Fe)SiO_3$ (OPv), having a significantly larger unit-cell volume as well as a more complex composition.

Methods

Our starting material was natural basalt glass from the Juan de Fuca Ridge. These samples contain 0.2 wt% water (H_2O), with all of the hydrogen being structurally bound as OH, as originally determined by spectroscopy and manometry [*Dixon et al., 1995*] and reconfirmed in the present experiments by Fourier-transform infrared (FTIR) absorption spectroscopy. Ground glass (< 1 μm particle size) was compressed in a diamond cell [*Mao et al., 1979*] to 30-65 GPa, and laser heated to temperatures of 1500-4000 K with a 20 W cw Nd-YAG laser [*Jeanloz and Kavner, 1996*]. A total of 22 high pressure samples were analyzed.

Pressures were determined through ruby fluorescence [*Mao et al., 1978*]; we were careful to perform laser-heating and subsequent analyses well away from the ruby calibrant. Pressures were measured both before and after heating, but only the post-heating pressures are reported here. Laser-heating converts the glass sample to the stable high-pressure crystalline phases, and the

pressures were systematically 5-10% lower after heating due to crystallization of the glass starting material and stress relaxation of the cell assembly. Pressure uncertainties reflect the variation between ruby chips. During heating, temperatures were determined via spectroradiometry [*Jeanloz and Kavner, 1996*], with measurements taken every 30-60 seconds and at least 5 temperature measurements taken per sample.

After synthesis, the samples were quenched to room temperature and then to zero pressure, and finally removed from the diamond cell. Synchrotron-based x-ray diffraction (SSRL beamline 10-2) was used to determine the crystalline phases present, and synchrotron-based FTIR (ALS beamline 1.4.3) was used to determine the water content of each phase. In comparison with benchtop FTIR, the advantages of synchrotron-based FTIR include a 2-3 order-of-magnitude enhancement in flux and reduction of the beam to a 10 micron diffraction-limited diameter [*Martin et al., 1998*]. This spot size is generally smaller than the hot-spot generated in the sample during laser heating [e.g., *Jeanloz and Kavner, 1996*]. Therefore, infrared absorption spectra can be collected from the same location in the sample that was heated, avoiding heterogeneities, unheated areas, and internal calibrants (ruby). The spectra from synchrotron-based FTIR consequently have greater signal-to-noise, and contain more reliable quantitative information than spectra collected from a benchtop system (Fig. 1).

The infrared spectra of all samples (except one) were collected before the x-ray diffraction patterns, avoiding possible radiation damage of metastable phases. We collected x-ray diffraction patterns on all but one sample (which was lost) at zero-pressure plus some samples at high pressure during and after heating, the results of which will be discussed elsewhere [*Panero and Jeanloz, in preparation*].

Angular-dispersive x-ray diffraction patterns were collected on image plates (λ=0.7277 Å; Fig. 2). Nearly full diffraction rings were collected, and reduced to one-dimensional patterns of intensity versus diffraction angle [*Nguyen and Jeanloz, 1993*]. The zero-pressure patterns were used to determine the phases synthesized in each experiment. Zero-pressure, unit-cell volumes were determined by Rietveld analysis [*Larson and Von Dreele, 1988*] and then used as a constraint

on the composition of each phase, and the relative volume proportions of each phase.

OH concentrations were then determined based on the Beer-Lambert law, using absorption coefficients previously reported for stishovite [*Pawley et al., 1993*]. The absorption coefficient has been adjusted by a factor of two to account for the use of non-polarized light, and an additional factor of three to account for the fact that Pawley et al. [*1993*] observed the OH bond to absorb only along the c axis. The small grain sizes of 50-200 nm found in these samples [*Funamori et al, 2000; Kesson et al., 1994*] are not expected to introduce significant problems in the analysis because the wavelength of the light (~3 μm) is much larger.

For each spectrum, the integrated OH-absorption (area under the peak) was calculated after subtracting out the background due to air and the contribution from unconverted glass. The thickness of the stishovite layer in the sample is estimated from the stishovite volume fraction times the crystalline thickness of the sample. Because the samples were initially glass and loaded into the diamond cell without a pressure medium, only the hottest portion of the sample was converted to the stable, high-pressure phases. No stishovite or perovskite is observed in x-ray diffraction patterns for samples heated to less than 1500 K at pressures between 30 and 60 GPa. Therefore, the thickness of the crystalline sample was determined to be that portion of the total sample thickness heated above 1500 K, according to the axial temperature distribution calculated by Panero and Jeanloz [*2001*] and assuming a thermal conductivity inversely proportional to temperature.

Uncertainty in the crystallization temperature does introduce uncertainty in our determinations of hydrogen content. The temperature of crystallization cannot be much higher than 1500 K because samples heated to 1600 (±75) K clearly exhibit the x-ray diffraction pattern of stishovite, but the crystallization temperature could be lower because temperatures below 1500 K are difficult to measure through spectroradiometry. Two samples heated to below this temperature exhibited no crystalline x-ray diffraction pattern. One had a measured temperature of 1450 (±150) K (Table 1, sample 822_5), and the other had a clearly visible hotspot on heating but the intensity of light was not great enough to accurately determine a temperature (sample 822M). If the crystallization temperature is, in fact, lower than 1500 K, then the inferred thickness of the

6

crystalline sample increases, decreasing the hydrogen concentration determined for each sample. If the crystallization temperature is 1200 K, for instance, our present estimates of hydrogen content would be decreased by a factor of 2 for a sample synthesized at a peak temperature of 1600 K. For a peak temperature of 2450 K, however, there is only a 12% decrease in the estimated hydrogen content. Notably, the lower-temperature data are more uncertain and the overall conclusions based on the data from the high-temperature runs are relatively unaffected. For the present analysis, the uncertainty in the temperature of crystallization has been taken conservatively to be 200 K. The overall uncertainty in total hydrogen concentration due to this source of error as well as uncertainties in the peak temperature and thickness of the sample have been evaluated assuming that each source of error is independent.

The infrared spectrum of the unconverted-glass portion of the sample changes after compression to high pressure and subsequent quenching to zero pressure without heating. Because of this, compressed glass standards were prepared at 30, 35, 40 and 55 GPa (all unheated), and were analyzed in parallel with the quenched samples, with the total amount of water contained in the glass assumed to be unchanged on compression without heating.

Results

We observe the sub-solidus phases of mid-ocean ridge basalt (MORB) heated between 30 and 60 GPa to be stishovite and the expanded (Mg, Ca, Fe, Al, Si)O_3-orthorhombic perovskite phase (OPvII), consistent with Funamori, et al.'s [*2000*] results. We find that samples undergoing partial melting exhibit a breakdown of OPvII to OPv (Mg,Fe,Al)SiO_3, Ca-perovskite, and an alumina-rich calcium ferrite (Al-CF; (Al, Si, Mg)O_4) structured phase upon temperature-quench [*Irifune et al., 1991*] (Fig. 2). We therefore consider Al-CF to be a quench phase formed from the high-pressure melt, compatible with previous reports on basalt-analogs laser heated at lower-mantle pressures [*Kesson et al., 1994*]. In all cases, the compositions of each phase can be taken as similar to those reported in Funamori et al., [*2000*]. No evidence of hydrous minerals, such as

7

phase D, superhydrous B, or phase B, was detected either through x-ray diffraction or infrared spectroscopy [*Pacalo and Parise, 1992*; *Yang et al., 1997*; *Cynn et al., 1996*; *Liu et al., 1998*]. Additionally, no evidence of a K-rich phase was found, likely due to the smaller quantities of K_2O in these samples (~0.15 wt%) compared to the 1.3 wt % K_2O present in experiments showing K-hollandite to be a coexisting phase under similar conditions as ours [*Wang and Takahashi, 1999*]. Some evidence for crystalline TiO_2 was found in the x-ray diffraction patterns (in the monoclinic baddeleyite phase), in quantities consistent with the 1.6 wt% TiO_2 in the starting sample [*Dixon et al., 1988*]. The presence of this minor phase does not have a significant bearing on the overall results presented here, although analogy with the low-pressure rutile phase suggests that small amounts of hydrogen may be present in the badelleyite structure [*Rossman and Smyth, 1990*].

All crystalline samples contained stishovite, and the OH concentration found in this phase is summarized in Table 1 and Figure 3. Based on diffraction results, stishovite makes up 20-40 volume% of the crystalline portion of the sample. Unless there was significant evidence of amorphization of other phases upon pressure quench (i. e., Ca-perovskite, and OPvII in sample 822-8), the volume fraction of stishovite in the sample is taken as the volume fraction obtained upon quench from Reitveld refinement of the x-ray diffraction patterns [*Larson and von Dreele, 1988*]. In the case of significant amorphization upon quenching, the volume fraction of stishovite in the sample was taken from refinement of diffraction patterns taken at pressure. In all cases, the uncertainty in the refinement resulted in 1-6% uncertainty in the volume fraction of stishovite in the sample, and this uncertainty has been included in our estimates of the uncertainties in the thickness and hydrogen content of each sample.

The thickness of stishovite in the samples is then determined by measuring the total thickness of the sample plus residual glass by measuring the gasket thickness after decompression. The fraction of sample which was crystallized is determined by measuring the peak temperature, and calculating the fraction of the sample which was heated above the crystallization temperature using numerical models of the axial gradients in the laser-heated diamond cell [*Panero and Jeanloz, 2001*]. The fraction of the crystalline sample that is stishovite is then derived from

8

Reitveld analysis. Each step involves uncertainties in the measurements, all of which have been included in the final uncertainty quoted for hydrogen concentration.

The concentration of hydrogen in stishovite increases with pressure by a factor of ~2 between 10 and 60 GPa under sub-solidus conditions (Fig. 3), a pressure range corresponding to a ~10% decrease in the unit-cell volume of stishovite. More significantly, the hydrogen content shows a marked increase with synthesis temperature over the pressure range of 30-38 GPa (Fig 3a), from about 100 ppm (wt) H_2O to 400 ppm (wt) H_2O in stishovite. Specifically, we attribute the jump at about 2800 K to the onset of partial melting in the sample. For the highest-temperature runs, there was clear visual evidence of melting during heating (i.e., fluid-like material motion in the hotspot). For those temperatures closer to 2800 K, melting was less obvious but some of the samples showed distinct round blebs upon quenching: identical to those quenched in the definitively melted samples. Samples heated to lower peak temperature demonstrate no such textures. The melting temperatures we observe for MORB (2780 (±50) K at 34 GPa for example) are quite consistent with those determined by Hirose et al. [*1999*] by a different method.

For those samples with evidence of melting, the hydrogen content in crystalline stishovite is 3-5 times greater than the concentrations in samples lacking evidence of melting. Moreover, the zero-pressure volume of stishovite formed in association with partial melt is consistently 0.3 (±0.15)% expanded relative to that of stishovite formed subsolidus, along with solid OPv II (13 wt % Al_2O_3), suggesting that stishovite incorporates aluminum when in the presence of an alumina-rich perovskite melt.

Indeed, the incorporation of aluminum into stishovite phase is well documented. TEM [*Kesson et al., 1994; Funamori et al., 2000*] and microprobe analyses [*Ono 1999*] show trace amounts of aluminum in the stishovite phase. Our inference that the concentration of Al impurities in stishovite increases upon partial melting of MORB at high pressures is supported by evidence that stishovite forms virtually alumina free under sub-solidus conditions [*Funamori et al., 2000*; *Panero et al., 2001*], whereas analyses by Kesson, et al. [*1994*] show that stishovite formed in association with Al-CF — which we ascribe to partial melting — contains as much as 3 mol %

Al$_2$O$_3$ at comparable pressures. The precision of *Funamori et al.*'s [*2000*] energy-dispersive analyses was inadequate for directly resolving the difference in Al content in sub-solidus *vs.* super-solidus stishovite, but their results are compatible with our conclusions [*Fujino et al.*, 1998].

Given that stishovite incorporates aluminum in the MORB samples that are partially melted at high pressures, it is likely that hydrogen is also incorporated into the stishovite due to the charge-coupled reaction

$$Si^{4+} = Al^{3+} + H^+ \qquad (1)$$

That is, the presence of an alumina-rich melt enhances the concentration of hydrogen impurities in the coexisting crystalline phase, with the heightened aluminum activity (in the melt, therefore partitioned into the crystalline phase on the solidus) inducing the uptake of hydrogen into the crystal, as we observe.

Despite all of the sources of error in absolute concentrations of hydrogen in stishovite, the *relative* shift in values that we observe as a function of pressure and temperature are quite significant. In particular, the increase of hydrogen content in the stishovite phase upon partial melting of the basalt assemblage is reliably documented in our experiments. Moreover, the absolute values of hydrogen concentration in sub-solidus stishovite are completely consistent with the lower-pressure measurements made by Pawley et al. [*1993*] (Fig 3b), who also found that the incorporation of 1% Al$_2$O$_3$ (wt) facilitates the uptake of hydrogen in stishovite.

We have considered alternative explanations for the enhanced abundance of H in stishovite upon partial melting of the high-pressure MORB assemblage. For example, temperature gradients can induce Soret diffusion in minerals [e. g., *Lesher 1986*], and there exist data showing that iron can diffuse away from the center of the laser-heated spot inside a diamond cell [*Heinz and Jeanloz, 1987*]. We note, however, that heating for different amounts of time, from under 5 seconds to over 15 minutes, results in no significant differences in hydrogen concentration in the experiments reported here (four points at 32 GPa and 2850 K in Fig 3a). In addition, when rastering the laser-heated spot across the sample at a peak temperature above the melting point, the highest OH concentrations were always found where the sample had been temperature quenched without

reheating; those regions of the sample that had been reheated to lower temperatures in the rastering process (due to lower temperatures at the edge of the hotspot) showed values comparable to the hydrogen content of unmelted samples. It is our conclusion that these rastering tests "reversed" the experiment by reheating a melted spot and recovering the lower-temperature distribution of hydrogen abundances, and that the increased hydrogen content observed in stishovite when in the presence of an alumina-rich melt is therefore sound.

Five samples contain OPvII and four contain OPv. However, no absorption band is found that can be attributed to an O—H stretch in the perovskite phase, despite the fact that this phase accounts for about 60-80% of the volume of the basalt samples. We examined the possibility that because of the larger zero-pressure volume of OPvII (about 167.9 Å^3) compared to OPv $MgSiO_3$-perovskite (162.3 Å^3), the frequency of the O—H vibration in our perovskite phase could be shifted relative to the 3483 and 3423 cm^{-1} bands of OPv [*Meade, et al, 1994*]. Like Bolfan-Casanova et al. [*2000*], however, we find no direct evidence of hydrogen incorporation into the perovskite structure (our sensitivity limit is estimated to be 50 ppm H_2O by weight). The contrast with *Meade et al.*'s [*1994*] results may be due to differences in the conditions under which the perovskites were synthesized. Recent results on Mg-perovskite [*Murakami et al., 2002*] indicate 0.2 wt% H_2O solubility when considering solid solutions with aluminum and iron, but with dramatically different IR spectra than was reported in Meade et al. [*1994*]. The inconsistencies between the experiments indicate that there may be a complex speciation of hydrogen in the perovskites, complicating the analysis of hydrogen incorporation in the perovksite phases synthesized in MORB samples.

Silicon is octahedrally coordinated in Al-CF, as in stishovite and perovskite, such that the OH stretching frequency for this phase should lie between 3000 and 3500 cm^{-1}. However, no unexplained peaks are observed in spectra of the four samples found to have the Al-CF phase. The lack of evidence for H could be due to (1) low abundances of incorporated hydrogen, (2) the small volume fraction of this phase (~10 wt%) or (3) the peak being obscured by the pressure-induced change in shape of the OH signature in glass.

Discussion and Conclusion

Accounting for a global water budget, Peacock [*1990*] finds that a significant amount of water either continues down toward the lower mantle or else underplates the crust. Unaltered crust contains as much as 0.7 wt % H_2O in nominally "anhydrous" minerals [*Delany et al., 1978*], and these are not expected to release water upon subduction as readily as is thought to be the case for the hydrated portion of the slab. The concentrations we have found in stishovite imply that at least some of the subducted hydrogen can be carried into the lower mantle without requiring hydrous minerals to be present in the slab.

Approximately 2×10^{23} kg of oceanic crust has been subducted over geological time (4×10^9 yr), assuming the present rate of subduction (5 cm/yr), length of subduction zones (46,000 km) and crustal thickness (6 km). This corresponds to 4×10^{22} kg of stishovite, which makes up about 0.2 of the high-pressure MORB assemblage. Taking a hydrogen concentration equivalent to 100 ppm (wt.) of H_2O, the subduction of stishovite within nominally anhydrous sub-oceanic crust has transported about 4×10^{18} kg of H_2O into the deep mantle. As much as three times this amount of water has been subducted into the lower mantle through anhydrous phases (up to 1.2×10^{19} kg), if we also consider the presence of up to 50 ppm H_2O in the perovskite phase. This corresponds to ~250-750 times the current water content of the atmosphere, or 0.3-0.9 percent of the hydrosphere, even before taking into account the presence of dense hydrous phases within the mantle. Faster rates of subduction in the geological past would imply even more effective recycling, and our experiments show that this is not counteracted by partial melting of the high-pressure assemblage (which leaves more hydrogen in the residual stishovite).

That the equivalent of an atmosphere's worth of water is recycled within 20 million years merely through subduction of "dry" oceanic crust provides a baseline for the potential significance of the Earth's deep interior as a reservoir for volatile molecules normally associated with the

hydrosphere. Indeed, the water content of the hydrosphere could be significantly affected by plate tectonics over the course of Earth history.

References

Albarède, F. and R. D. van der Hilst , New Mantle Convection Model May Reconcile Conflicting Evidence, *Eos*, *80*, 535,537-539, 1999.

Alt, J. C. and D. A. H. Teagle, Hydrothermal alteration and fluid fluxes in ophiolites and oceanic crust, *in* Dilek, Y., Moores, E. M., Elthon, D., and Nicolas, A., eds, Ophiolites and Oceanic Crust: New insights from field studies and the Ocean Drilling Program: Boulder, CO, Geological Society of America Special Paper 349, p. 273-282, 2000.

Bell, D. R., and G. R. Rossman, Water In Earth's Mantle - the Role Of Nominally Anhydrous Minerals, *Science*, *255* (5050), 1391-1397, 1992.

Bolfan-Casanova, N., H. Keppler, and D. C. Rubie, Water partitioning between nominally anhydrous minerals in the MgO-SiO2-H2O system up to 24 GPa: implications for the distribution of water in the Earth's mantle, *Earth and Planetary Science Letters*, *182* (3-4), 209-21, 2000.

Cynn, H., A.M. Hofmeister, P.C. Burnley, and A. Navrotsky, Thermodynamic properties and hydrogen speciation from vibrational spectra of dense hydrous magnesium silicates, *Physics and Chemistry of Minerals*, *23* (6), 361-76, 1996.

Delany, J. R., D. W. Muenow, and D. G. Graham, Abundance and distribution of water, carbon, and sulfur in the glassy rims of submarine pillow basalts, *Geochim. Cosmochim. Acta 42*, 309-23, 1978.

Dixon, J. E., E. M. Stolper, and J. R. Holloway, An experimental study of water and carbon dioxide solubilities in mid-ocean ridge basaltic liquids. Part 1: Calibration and solubility models, Journal of Petrology, 36, 1607-1631, 1995.

Fujino, K., N. Miyajima, T. Yagi, T. Kondo, and N. Funamori, Analytical electron microscopy of the garnet-perovskite transformation in a laser-heated diamond anvil cell, in *Properties of Earth and Planetary Materials at High Pressure and Temperature, Geophys. Momgr. Ser.,* vol. 101, ed. M. H. Manghnani and T. Yagi, pp. 409-417, AGU, Washington, D. C., 1998.

Funamori, N., R. Jeanloz, N. Miyajima, and K. Fujino, Temperature-Dependent Mineral Assemblages of Basalt at Lower-Mantle Conditions, *Journal of Geophysical Research*, *105* (B11), 26037-26043, 2000.

Grand, S. P., R. D. van der Hilst, and S. Widiyantoro, Global seismic tomography: A snapshot of convection in the Earth, *Geol. Soc. Am. Today, 7* (1) 1997.

Heinz, D.L. and R. Jeanloz, Temperature measurements in the laser-heated diamond cell, in *High-pressure research in mineral physics*, edited by M.H.S. Manghnani, Y., pp. 113-127, American Geophysical Union, Tokyo, 1987.

Hirose, K., Y. Fei, Y. Ma, and H-K. Mao, The fate of subducted basaltic crust in the Earth's lower mantle, *Nature*, *397* (6714), 53-6, 1999.

Ito, E., D. M. Harris, A. T. Anderson, Alteration of oceanic crust and geologic cycling of chlorine and water, *Geochim. Cosmochim. Acta, 47*, 1613-1624, 1983.

Irifune, T., K. Fujino, and E. Ohtani, A new high-pressure form of $MgAl_2O_4$, *Nature, 349*, 409-11, 1991.

Jeanloz, R. and A. Kavner, Melting criteria and imaging spectroradiometry in laser-heated diamond-cell experiments, in Developments in High-Pressure, High-Temperature Research and the Study of the Earth's Deep Interior, pp. 1279-305, *Philosophical Transactions of the Royal Society London*, London, UK, 1995.

Kellogg, L.H.H., B.H. Hager, and R. D. van der Hilst, Compositional stratification in the deep mantle, *Science*, *283* (5409), 1881-4, 1999.

Kesson, S. E., J. D. Fitz Gerald, and J. M. G. Shelly, Mineral chemistry and density of subducted basaltic crust at lower-mantle pressures, *Nature, 372*, 767-769, 1994.

Kuramoto, K. and T. Matsui, Partitioning of H and C between the mantle and core during the core formation in the Earth: its implications for the atmospheric evolution and redox state of early mantle, *Journal of Geophysical Research*, *101*, 14909-32, 1996.

Larson, A. C. and R. B. Von Dreele, GSAS manual, report LAUR 86-748, Los Alamos National Laboratory, 1988.

Lesher, C.E., Effects of silicate liquid composition on mineral-liquid element partitioning from Soret diffusion studies, pp. 6123-41, 1986.

Liu, L. G., C. C. Lin, T. Irifune, T. P. Mernagh, Raman study of phase D at various pressures and temperatures, *Geophysical Research Letters, 25*, 3453-3456, 1998.

Lu, R. and H. Keppler, Water solubility in pyrope to 100 kbar, *Contrib. Mineral. Petrol. 129*, 35-42, 1997.

Mao, H.K., P.M. Bell, J.W. Shaner, and D.J. Steinberg, Specific volume measurements of Cu, Mo, Pd, and Ag and calibration of the ruby R_1 fluorescence pressure gauge from 0.06 to 1 Mbar, *Journal of Applied Physics*, *49* (6), 3276-83, 1978.

Mao, H.K., P.M. Bell, K.J. Dunn, R.M. Chrenko, and R.C. DeVries, Absolute pressure measurements and analysis of diamonds subjected to maximum static pressures of 1.3-1.7 Mbar, *Review of Scientific Instruments*, *50* (8), 1002-9, 1979.

Martin, M. C., Wayne R. McKinney, Proceed. Mater. Res. Soc., 524, 11 (1998). LBNL-41803, LSBL-460."The First Synchrotron Infrared Beamlines at the Advanced Light Source: Microspectroscopy and Fast Timing"

Meade, C., J.A. Reffner, and E. Ito, Synchrotron infrared absorbance measurements of hydrogen in $MgSiO_3$ perovskite, *Science*, *264* (5165), 1558-60, 1994.

Murakami, M., K. Hirose, H. Yurimoto, S. Nakashima, N. Takafuji, Water in Earth's Lower Mantle, *Science, 295*, 1885-7, 2002.

Nguyen, J. H. and R. Jeanloz, A computer program to analyze x-ray diffraction films, *Review of Scientific Instruments, 64*, 3456-61, 1993.

Ono, S., High temperature stability limit of phase egg, AlSiO3(OH), *Contrib. Mineral. Petrol.*, *137*, 83-89, 1999.

Pacalo, R. E. G., and J. Parise, Crystal structure of superhydrous B, a hydrous magnesium silicates synthesized at 1400°C and 20 GPa, *American Mineralogist, 82*, 681-684, 1992.

Panero, W. R., L. R. Benedetti, and R. Jeanloz, Equation of state of stishovite and interpretation of SiO_2 shock compressions data, *in review*.

Panero, W., and R. Jeanloz, Temperature gradients in the laser-heated diamond cell, *Journal of Geophysical Research, 106*, 6493-6498, 2001a.

Pawley, A.R., P.F. McMillan, and J.R. Holloway, Hydrogen in Stishovite, with Implications for Mantle Water Content, *Science*, *261*, 1024-1026, 1993.

Peacock, S.M., Fluid processes in subduction zones, *Science*, *248* (4953), 329-37, 1990.

Righter, K., and M.J. Drake, Effect of water on metal-silicate partitioning of siderophile elements: a high pressure and temperature terrestrial magma ocean and core formation, *Earth and Planetary Science Letters*, *171* (3), 383-99, 1999.

Rossman, G. R. and J. R. Smyth, Hydroxyl contents of accessory minerals in mantle eclogites and related rocks, *American Mineralogist, 75*, 775-780, 1990.

Schmidt, M.W. Experimental constraints on recycling of potassium from subducted oceanic crust, *Science, 272*,1927-30, 1996.

Schmidt, M.W., and S. Poli, Experimentally based water budgets for dehydrating slabs and consequences for arc magma generation, *Earth and Planetary Science Letters*, *163* (1-4), 361-79, 1998.

Tackley, P.J., Mantle Convection and Plate Tectonics: Towards an Integrated Physical and Chemical Theory, *Science*, *288*, 2002-2007, 2000.

Thompson, A.B., Water in the Earth's upper mantle, *Nature, 358*, 295-302, 1992.

Van der Voo, R., W. Spakman, and H. Bijwaard, Mesozoic subducted slabs under Siberia, *Nature, 397*, 246-9, 1999.

Wang, W. and E. Takahashi, Subsolidus and melting experiments of a K-rich basaltic composition to 27 GPa: Implications for the behavior of potassium in the mantle, *American Mineralogist, 84*, 357-361, 1999.

Williams, Q. and R. J. Hemley, Hydrogen in the Deep Earth, *Annu. Rev. Earth Planet Sci., 29*, 365-

418, 2001.

Yang, H., C. T. Prewitt, D. J. Frost, Crystal structure of the dense hydrous magnesium silicate, phase D, *American Mineralogist, 82*, 651-654, 1997.

Table 1
Experimental Results

Sample	Post-heat Pressure (GPa)	Peak Temperature (K)	Melt?	Quenched Phases	C_{OH} (ppm wt) in St	heating style
817_8	32.4±2	2850±75 (<5 sec)	yes (Q)	St, Al-CF, OPv	463±59	spot
		2850±75 (30 sec)	yes (Q)		487±62	spot
		2850±75 (3 minutes)	yes (Q)		417±53	spot
		2850±75 (15 minutes)	yes (Q)		453±58	spot
822_5	48±3	1450±150	no	none	N/A	raster
822_8	38.9±2	1600±75	no	St	76±50	raster
822M	35.2±3	not measurable	no	none	N/A	raster
824M	33.5±2	3522±160	yes (V+Q)	St, Al-CF, OPv	403±41	raster
826M	30.4±2	3200±100	yes (V+Q)	St, Al-CF, OPv	406±44	raster
827M	30±4	2155±240	no	St, OPvII	129±30	spot
116_6	30±3	2013±150	no	St, OPvII	208±51	raster
117a_6	38±2	1956±230	no	St, OPvII	81±25	spot
117b_6	36.9±2	2755±150	no (Q)	St, OPvII	85±11	raster
1115a_6	51.3±2.3	2210±208	no	St, OPvII	235±50	raster
1116a_5	62.9±5	2452±131	no	St, OPvII**	200±33	raster
		3979±193	yes (V+Q)	St, Al-CF, OPv**	393±36	raster
Standards/Controls:						
1023Mb	28.3	no heat				
1024Ma	40	no heat				
1031Ma	35	no heat				
1114a_6	55	no heat				
117c_6	25	no heat (dry synthetic)				
1114b_6	32.9 (±1)	2130 ± 150 (dry synthetic)				

Q - quench textures (or lack) present
V - visual observation of liquid motion during heating
Phase abbreviations: St - stishovite; Al-CF - alumina-rich calcium ferrite phase; OPv - (Mg,Fe,Al) orthorhombic perovskite; OPvII - (Mg, Fe, Al, Ca) orthorhombic perovskite
** sample lost, assumed based on similarity of conditions to samples 827M and 824M

Figure Captions

Figure 1:

Spectra of a sample synthesized at 32 ($\pm$2) GPa and 2850 ($\pm$150) K, comparing results from a synchrotron-based system (black, Advanced Light Source beamline 1.4.3; Nicolet Magna 760 with KBr beamsplitter and an MCT detector) to the spectrum from a lab-based system (gray, Bruker IFS-66v using a CaF_2 beamsplitter and an InSb detector). The collection time for the synchrotron-based system was about 2 minutes (256 scans, top), compared to about 7 hours (60000 scans, bottom) for the lab-based system. While both show a distinct peak at 3111 cm^{-1} corresponding to OH vibrations in stishovite, the synchrotron-based spectrum has a better signal-to-noise ratio, as well as better spatial resolution. There is no detectable absorption at 3450 cm^{-1}, where OH in Mg-perovskite is expected to absorb. A control experiment was performed on a dry, synthetic basalt glass starting material (sample 1114b_6); synthesis conditions were 33 ($\pm$1) GPa and 2130 ($\pm$150) K. No absorption features were found in the 3000 - 3500 cm^{-1} region for this sample (thin line, bottom), again collected by synchrotron FTIR.

Figure 2:

Reitveld refinement of x-ray diffraction patterns from samples (top) 117b_6 and (bottom) 824M upon pressure quench. Crosses are the data (background subtracted) and the lines are the fits. Below each diffraction pattern is the residual and expected location of diffraction peaks for the phases in each sample. The refinement for sample 117b_6 has a χ^2 =6.8, with a sample composition of 32.8 ($\pm$2.1) wt % stishovite and 67.2 ($\pm$1.0) wt % OPvII. The refinement for sample 824M has a χ^2 = 5.1, with the sample containing 28.7 ($\pm$1.4) wt % stishovite, 58.3 ($\pm$1.0) wt % OPv and 13.0 ($\pm$1.4) wt % Al-CF.

Figure 3:

The OH concentration in stishovite as a function of temperature (a; data between 30-38 GPa) and

pressure (b). Solid symbols indicate concentrations in stishovite formed subsolidus; open symbols for samples that have undergone partial melting; triangle is the point determined by Pawley et al. [*1993*]. Hydrogen concentration increases by a factor of 3-5 with the onset of melting [*Hirose et al., 1999*]. Sub-solidus, the hydrogen content in stishovite shows a slight increase with pressure.
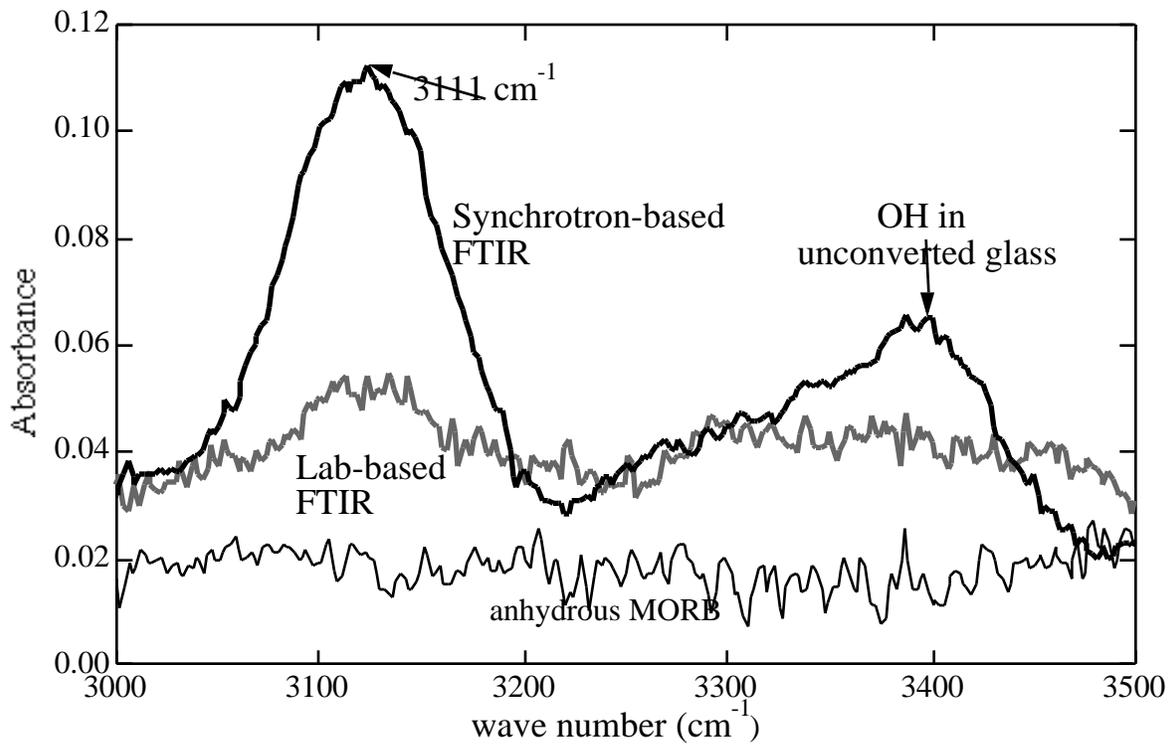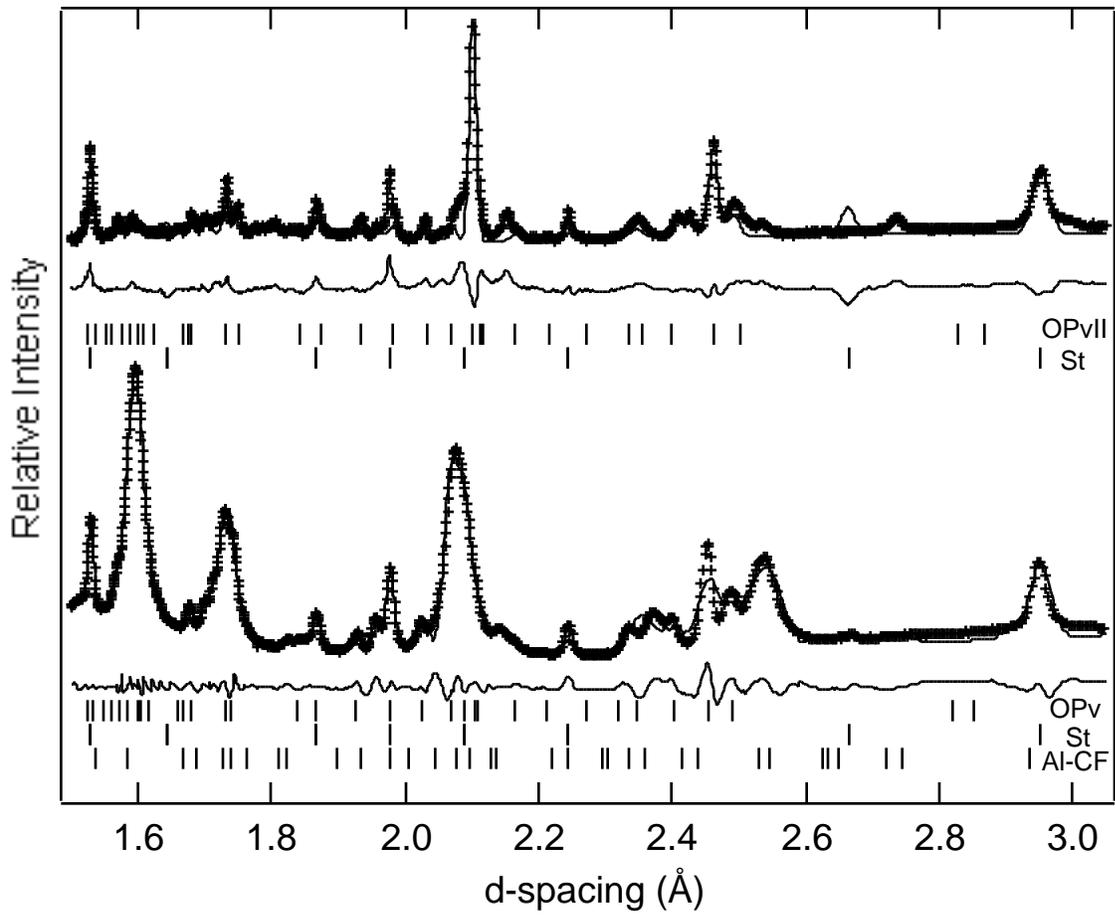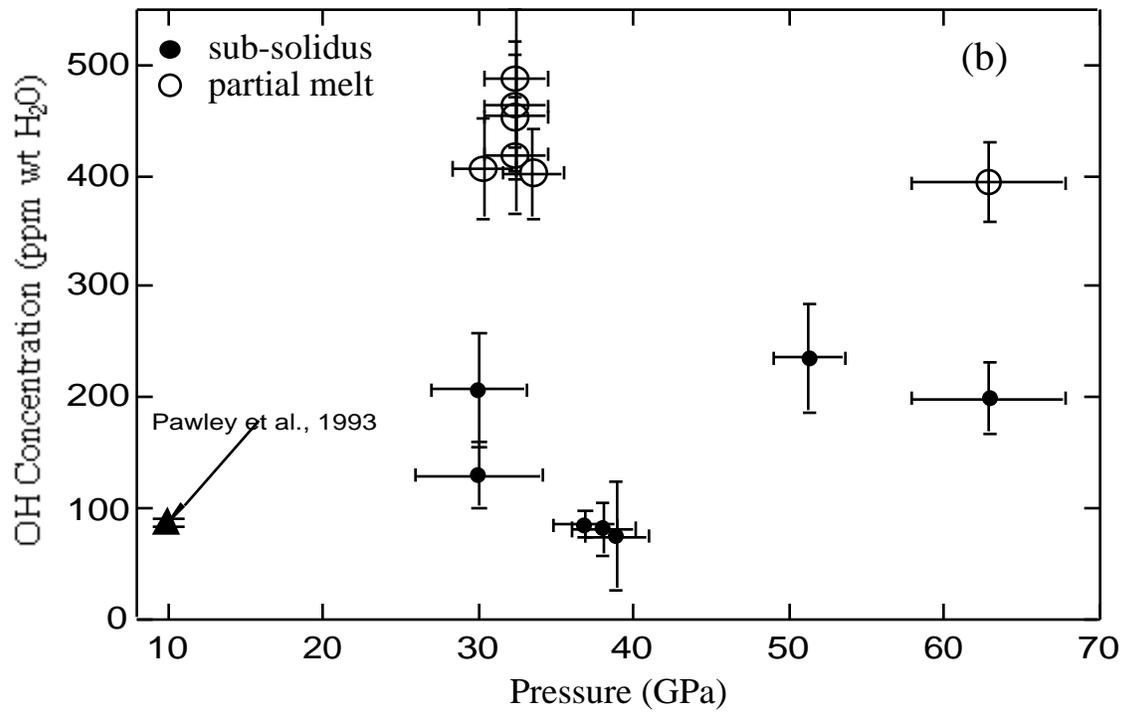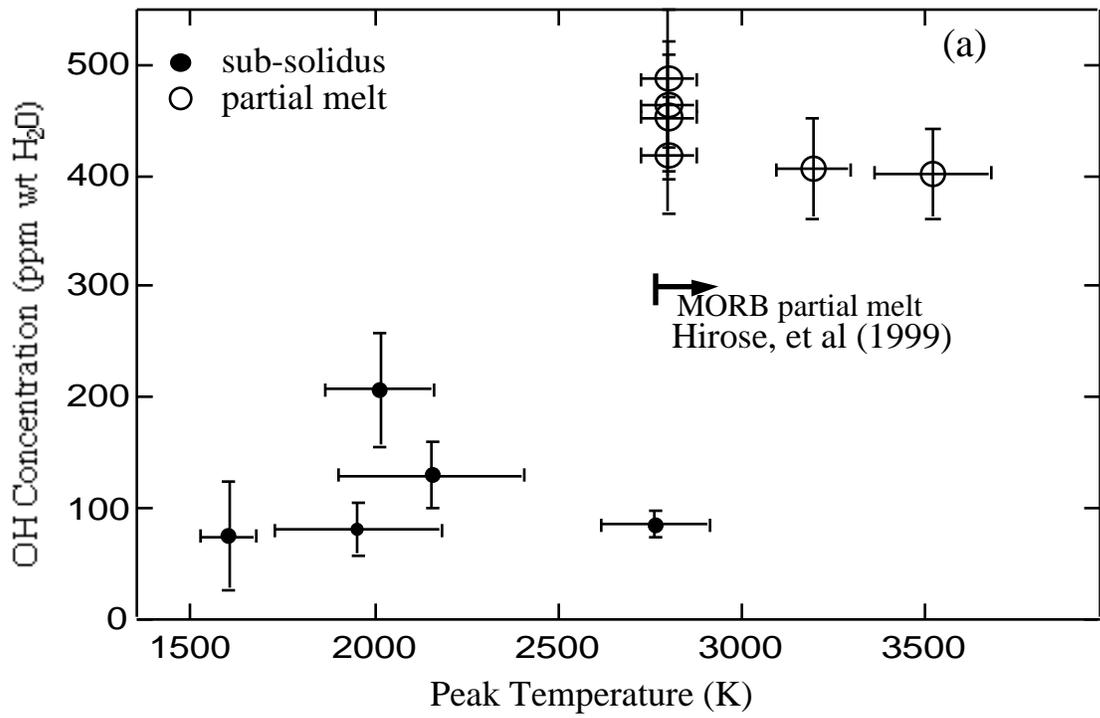
Figure 1

Figure 2

Figure 3